Evidence for hidden order in a nonlinear model elastic system

OPEN ACCESS
IOP Publishing

Letters
Journal of Physics: Condensed Matter

J. Phys.: Condens. Matter **31** (2019) 10LT01 (6pp)
https://doi.org/10.1088/1361-648X/aafcfe

Letter

Evidence for hidden order in a nonlinear model elastic system

P A Deymier and K Runge

Department of Materials Science and Engineering, 1235 E. James E Rogers Way, University of Arizona, Tucson, AZ 85721, United States of America

E-mail: deymier@email.arizona.edu and krunge@email.arizona.edu

Received 15 October 2018, revised 17 December 2018
Accepted for publication 9 January 2019
Published 18 January 2019

Abstract

Hidden order may arise in strongly correlated systems even if there is an apparent lack of long-range order as measured by local order parameters. This phenomenon has been essentially associated with topological order in quantum systems. Here, we demonstrate the emergence of hidden order in a 1D non-linear classical mechanical system that supports rotational degrees of freedom. The potential energy of the model system creates a bistable system for which hidden order emerges with the introduction of a biquadratic term. To our surprise, we discover that varying the strength of the biquadratic term leads to four distinct phases quantified by the behaviors of the Néel and string order parameters. Three of these phases are locally disordered. Hidden order is identified by a string order parameter that shows correlations with significantly longer range than the Néel order parameter. The hidden order correlation length diverges as the kinetic energy of the system is lowered with a critical exponent ~0.5. The observation of hidden order in a mechanical system reveals that instability and non-linearity may play critical roles in the generation of nonlocal long-range correlations in apparently locally disordered systems.

Keywords: hidden order, nonlinear mechanics, topological order, classical mechanics

1. Introduction

Recently, analogies have been drawn between wave behavior in elastic media and quantum phenomena [1]. For instance, acoustic and elastic analogues of topological insulators have been demonstrated [2–4]. While topological insulator-like acoustic/elastic systems essentially associate with linear band structure characteristics, another form of topological phenomenon may result from strong correlations and nonlinearity, namely topological order. Topological order is a phenomenon observed in strongly correlated quantum many-body systems [5, 6]. One attribute of topological order in quantum matter, such as the Haldane phase in spin-1 chains, is their apparent lack of long-range order (i.e. local order parameters have the characteristics of disordered liquids) but they actually exhibit long-range correlation patterns [7, 8]. In elastic systems, geometry and/or nonlinearity can be sources of order or disorder. Geometric frustration in a two-dimension acoustic network of waveguides can give rise to disordered configurations [9]. However, buckling can induce complex ordered patterns in statically loaded geometrically frustrated triangular cellular structures [10]. Here, we report a one-dimensional (1D) non-linear elastic dynamical system which potential energy allows buckling and then examine the consequences of including a biquadratic term. With this inclusion the system now supports locally disordered phases. Quantification of order through local and nonlocal order parameters provides evidence for the existence of a nonlocal hidden order reminiscent of that observed in topological phases. In particular, we reveal a hidden nonlocal string ordered (SO) phase analogous to that identified in quantum magnetic systems [11].

2. Model system

We consider a 1D system composed of subsystems coupled through nearest neighbor interactions. The state of each subsystem 'i' is characterized by a continuous angular variable θ_i. We introduce the following unperturbed model potential energy:

$$E_0\left(\{\theta_i\}\right) = A\sum_i \theta_i\theta_{i+1} + \frac{1}{2}B\sum_i \theta_i^2 + C\sum_i \cos\theta_i. \quad (1)$$

The constants A, B, and C are positive. The third term in equation (1) can be rewritten as

$$\frac{1}{2}B\sum_i \theta_i^2 = \frac{1}{2}A\sum_i \theta_i^2 + \frac{1}{2}A\sum_i \theta_{i+1}^2 + \frac{1}{2}\left(B-2A\right)\sum_i \theta_i^2. \quad (2)$$

Combining the first two terms of equation (2) with the first term of equation (1) leads to

$$E_0\left(\{\theta_i\}\right) = \frac{1}{2}A\sum_i \left(\theta_i+\theta_{i+1}\right)^2 + \frac{1}{2}\left(B-2A\right)\sum_i \theta_i^2 + C\sum_i \cos\theta_i. \quad (3)$$

We choose $B-2A>0$ so that the potential energy of the system displays bistability for positive and negative values of θ_i. We now introduce a nonlinear term which when combined with the first term of equation (3) resembles the AKLT extension of the 1D Heisenberg spin model [12]. This model system can be understood physically as a nonlinear elastic system.

$$E\left(\{\theta_i\}\right) = E_0\left(\{\theta_i\}\right) + E'\left(\{\theta_i\}\right);\; E'\left(\{\theta_i\}\right) = D\sum_i \left(\theta_i\theta_{i+1}\right)^2. \quad (4)$$

The first term of equation (3) represents the lowest-order contribution to the potential energy of a 1D block-spring model that supports rotational motion. This model is based on a discrete linear 1D micromechanics model that includes rotational degrees of freedom, θ_i [13, 14]. This model consists of an infinite chain of square block elements which opposite corners are connected via harmonic springs (see figure 1). The other two terms of equation (3) represent contributions to the potential energy of articulated arms under an axial load and a torsional spring located at each articulation, respectively. In this mechanical interpretation of equation (3), each block is attached to the articulation of the arm. Since, an arm can undergo sideways deflection or buckling, the orientation of the corresponding block exhibits bistability [15]. For the sake of simplicity, we assume that the arm can move laterally to maintain a constant distance between blocks thus neglecting the dynamics of displacements. The first term in equation (1) favors an antiferromagnetic-like arrangement of the orientations i.e. angles with alternating signs along the lattice. The biquadratic term, $E'\left(\{\theta_i\}\right) = \sum_i \left(D\theta_i^2\right)\theta_{i+1}^2 = \sum_i \frac{1}{2}K(|\theta_i|)\theta_{i+1}^2$ may be visualized as resulting from a feedback mechanism which modifies the stiffness of the torsional spring associated with block '$i+1$' based on the magnitude of the angular variable of the preceding block 'i', namely $K(|\theta_i|)$. An experimental system using magnetoelasticity [16] or photoelasticity [17] could potentially be used to realize this combination of bistability and nonlinear feedback. The biquadratic term can push the system away from the antiferromagnetic-like arrangement depending on its strength, D.

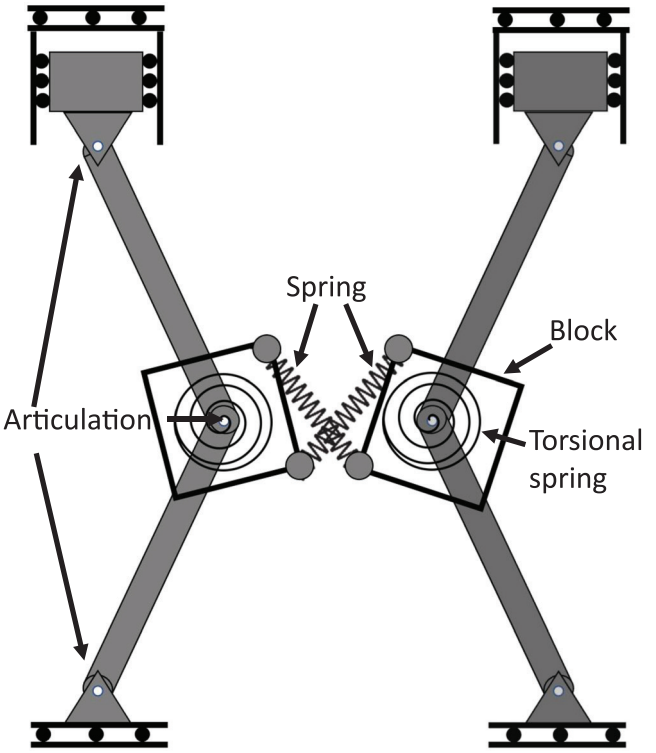

Figure 1. Schematic representation of two elements of a 1D block-spring model attached to axially loaded articulated arms with torsional springs.

We now introduce the Lagrangian, $L\left(\{\theta_i\},\left\{\frac{\mathrm{d}\theta_i}{\mathrm{d}t}\right\}\right) = \frac{1}{2}\sum I\left(\frac{\mathrm{d}\theta_i}{\mathrm{d}t}\right)^2 - E\left(\{\theta_i\}\right)$, from which one can derive the model system dynamical equation:

$$I\frac{\mathrm{d}^2\theta_i}{\mathrm{d}t^2} = -A\left(\theta_{i+1}+2\theta_i+\theta_{i-1}\right) - \left(B-2A\right)\theta_i + C\sin\theta_i - 2D\theta_i\left(\theta_{i+1}^2+\theta_{i-1}^2\right). \quad (5)$$

In equation (5), I, is the moment of inertia of a block. For the reference system, E_0, the equilibrium orientations of the bistable arm $\pm\theta_c$ are given by the condition $\left(B-2A\right)\theta_c = C\sin\theta_c$. Considering small deviations about an antiferromagnetic-likestate: $\theta_{i+1} = \pm\theta_c + \delta_{i+1}, \theta_i = \mp\theta_c + \delta_i$, and $\theta_{i-1} = \pm\theta_c + \delta_{i-1}$, the first term in equation (5) would reduce to the small deviation limit $-A\left(\delta_{i+1}+2\delta_i+\delta_{i-1}\right)$.

3. Results

We investigate the model system with the biquadratic term, E', by solving equation (5) numerically. There exist sets of parameters $\{I, A, B, C, D\}$ for which the nonlinear elastic system exhibits a number of 'phases' which will be subsequently characterized through order parameters.

In particular, we consider the following parameters: $A/I = 0.5\times10^{-2}\,\mathrm{s}^{-2}$, $B/I = 2\times10^{-2}\,\mathrm{s}^{-2}$, $C/I = 0.15\,\mathrm{s}^{-2}$ with $d = D/I$ taken as a variable. With these parameters, $\theta_c = 2.76$ radians. Equation (5) is solved using the

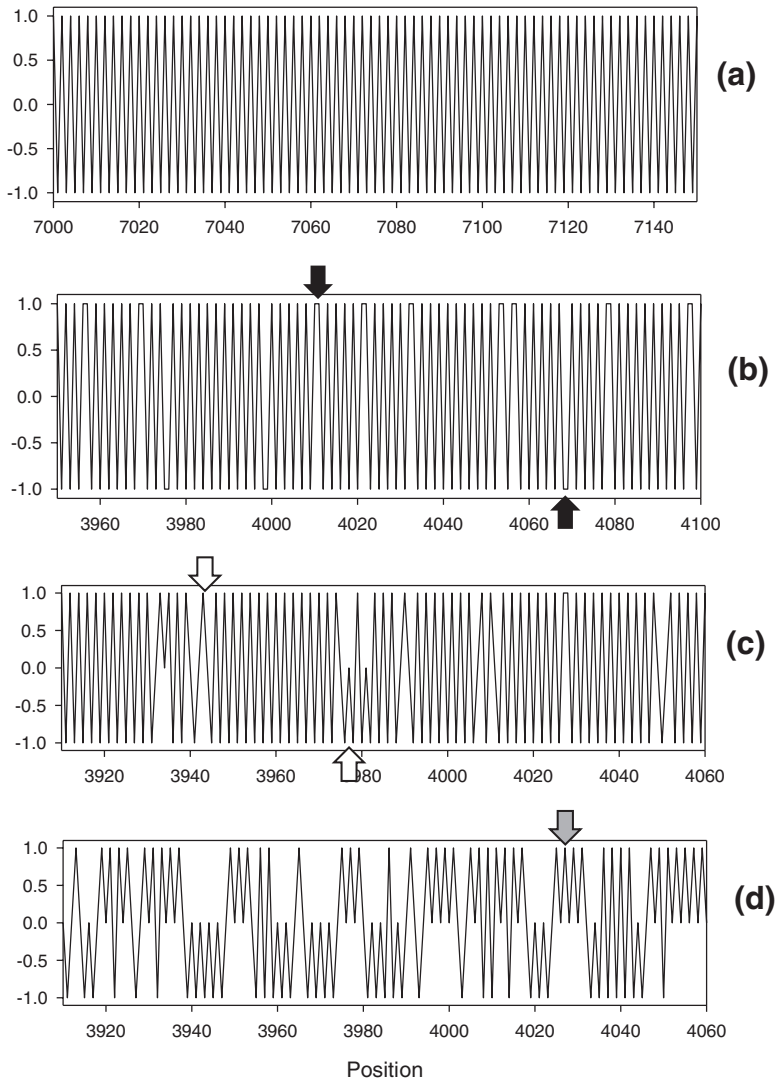

Figure 2. Sections of the annealed structures for (a) the antiferromagnetic-like (AF) phase ($d = 0$), (b) the spin liquid-like (SL) phase ($d = 0.004$), (c) string ordered (SO) phase ($d = 0.005$) and (d) disordered (D) phase ($d = 0.0055$). In (b) the black arrows mark from left to right two SS features. In (c) the open arrows identify from left to right the features $-0+-$ and $-0-$ the gray arrow in (d) shows one $+0+0+0+$ sequence. The position is defined by the site index.

conventional Verlet's algorithm with a small time integration step of $\Delta t = 2.5 \times 10^{-2}$ s guaranteeing energy conservation for all the conditions studied here. The initial conditions are chosen to be an antiferromagnetic-like arrangement of angular degrees of freedom with small random deviations $\theta_i = (-1)^i \theta_c + 2.5 \times 10^{-3} \times r$, where r is a random number between -1 and 1. The system contains 11 000 subsystems and periodic boundary conditions are used to avoid free ends such that it is in the large system limit. Simulations are performed using 3.1 million time-integration steps. The system is annealed by following the standard protocol of velocity rescaling i.e. by decreasing the angular velocities of the blocks by factors of 10 at 2, 2.5, 2.7, 2.8, 2.9, 2.95, and 2.975 million steps. The annealed structure is analyzed using the usual Néel order parameter and the string order parameter of den Nijs and Rommelse [18]. These are calculated as:

$$O_{\text{Néel}} = (-1)^{|j-i|} \hat{\theta}_i \hat{\theta}_j \tag{6}$$

$$O_{\text{String}} = -\hat{\theta}_i (-1)^{\sum_{l=i+1}^{j-1} \hat{\theta}_l} \hat{\theta}_j. \tag{7}$$

In equations (6) and (7) we have discretized the continuous angular variable as follows $\hat{\theta}_k = \theta_k / |\theta_k|$ if $|\theta_k| > 0.95$ and $\hat{\theta}_k = 0$ otherwise. The $\hat{\theta}_i$ takes on the values $+1, 0, -1$. The choice of the threshold 0.95 radians is motivated by the location of the inflection points of the bistable arm. In the model the inflection points are given by $(B - 2A) = -C \cos \theta_I$ corresponding to $\theta_I \cong 1.5$ rad. A threshold of 0.95 offers a more stringent margin in defining an equilibrium value of $\theta_i = 0$. Although called order parameters, $O_{\text{Néel}}$ and O_{String}, differ from the usual thermodynamics order parameters, such as the magnetization for ferromagnets $\sum_i \hat{\theta}_i$ or the staggered magnetization for antiferromagnet, i.e. $\sum_i (-1)^i \hat{\theta}_i$. These latter quantities are local in the sense that they only depend on on-site values of the variable $\hat{\theta}_i$ equations (6) and (7) are

effectively correlation functions that measure the relative order between different sites. These correlation functions are most pertinent to characterize topological phases with long-range correlation patterns.

To aid in the analysis of the states of the simulation, we introduce three classifications for consecutive blocks which may have alternating signs (AS), e.g. $+-$ or $-+$, same signs (SS), e.g. $++$ or $--$, or contain a zero (ZS), e.g. $0-$, $0+$, etc. Note that for the pure Néel ordered state all consecutive blocks have AS ordering.

We identified four 'phases' based on the behavior of the order parameters. For $d \in [0, d_1]$ with $d_1 \cong 0.001$ s^{-2} i.e. for very small biquadratic terms in equation (3), the annealed 1D system is long range ordered and $O_{\text{Néel}} = O_{\text{String}} = 1$. $\hat{\theta}_i = (-1)^i$ and the state of the annealed system resembles a Néel ordered antiferromagnetic (AF) state (see figure 2(a)). The unannealed system supports wave-like excitations which correspond to small deviations from the perfect antiferromagnetic-like order. This phase will be denoted the AF phase. For $d \in [d_1, d_2]$ where $d_2 \sim 0.0045$ s^{-2}, the annealed structure has antiferromagnetic-like character but now supports SS type structural features (see figure 2(b)). These are two adjacent sites with $\hat{\theta}_i = \hat{\theta}_{i+1} = \pm 1$. These features may be represented by the sequences $+-++-+$ or $-+--+-$ (see figure 2(b)). This phase does not support $\hat{\theta}_k = 0$ states. The system is not Néel ordered as the SS features appear to be randomly distributed along the 1D system. The antiferromagnetic-like correlations appear to be short ranged (as seen in figure 3(a)) and $O_{\text{Néel}} = O_{\text{String}}$. This phase is similar to a spin liquid with only short-range correlations; we denote it the SL phase. For $d \in [d_2, d_3]$ with $d_3 \sim 0.0051$ s^{-2}, the annealed structure supports very few SS type features but exhibits a number of ZS type sites. The number of zero sites increases with increasing value of d. Remarkably, there is some level of correlation between non-zero sites separated by a zero (figure 2(c)). In particular, the antiferromagnetic order appears likely to be conserved across zeros, that is one can represent these states by sequences of the form $-+0-+$ or $+-0+-$. This level of correlation is apparent in figure 3(b) where $O_{\text{String}} > O_{\text{Néel}}$ over an extended range (~40 sites). There is hidden order over this range extending well beyond the Néel correlation that O_{String} reveals. This phase does not display infinite long-range order as in the AF phase but there is string-like correlation over quite significant finite distances. Two types of additional structural features appear to be responsible for the finite range of string correlations, namely a few rare SS features and ZS features separated by one non-zero site which appears to break the AF order. These latter features may be represented for example by sequences of the form $-+0+0+-$, $+-0-0-+$ or $-+0+0-+$. We denote the phase with strong string correlation the string ordered (SO) phase. In a squeezed space, constructed by removing all sites with a '0' from the chain, the system would exhibit finite-range antiferromagnetic order. When $d > d_3$, the system contains enough zeros separated by one non-zero site to break the string-like order. This type of structure is illustrated in figure 2(c). This structure is constituted of short segments composed of $+0+$ or $-0-$ elements with interspersed $+0-$ or $-0+$ elements. Both order parameters $O_{\text{Néel}}$ and O_{String} are very short range as shown in figure 3(c). We call this disordered phase the D phase. The observed phases as a function of the parameter d, are summarized in the phase diagram of figure 4.

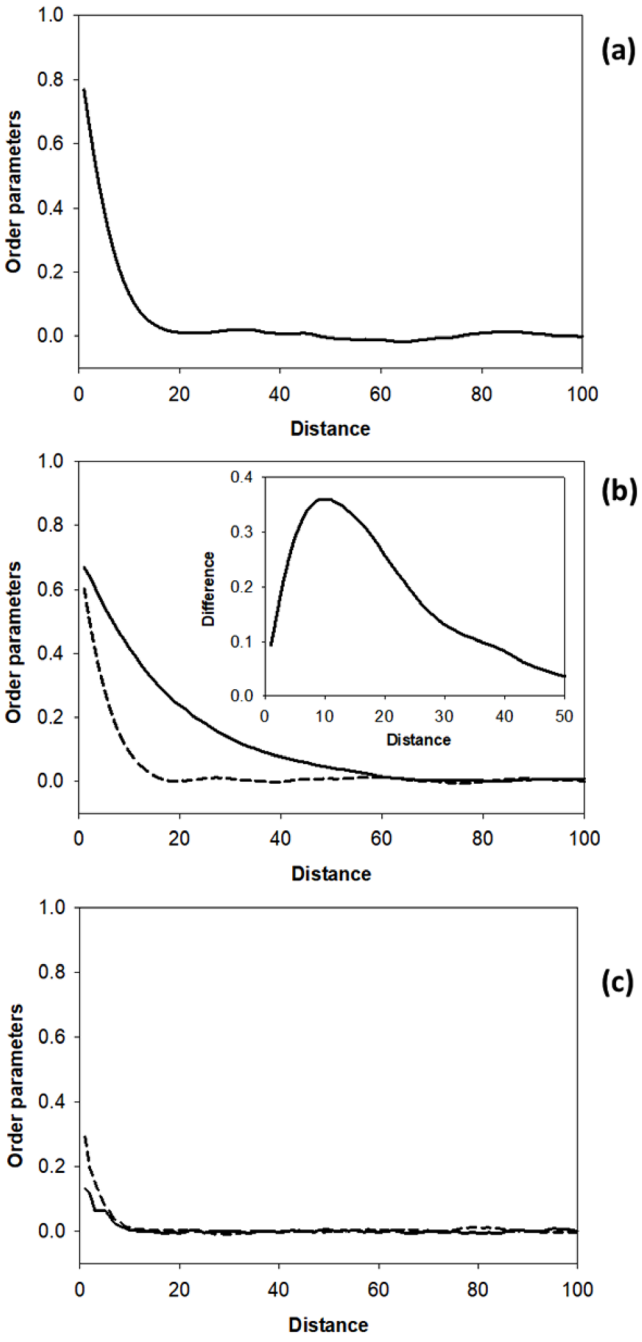

Figure 3. Néel order parameter (dashed line) and string order parameter (solid line) averaged over (a) four annealed structures of the spin liquid-like (SL) phase ($d = 0.004$), (b) eight string ordered (SO) phase structures ($d = 0.005$) and (d) four annealed structures of the disordered (D) phase ($d = 0.0055$). For (a), the two order parameters completely overlap. The inset in (b) represents the difference in order parameters and shows long range string order extending up to ~40 site spacings. The standard deviation on the calculated averages does not exceed 0.05. The distance is measured in number of site spacings.

Figure 4. Schematic illustration of the phase diagram. The observed phases are the AF phase, SL phase, SO phase and the D phase. d is a measure of the strength of the biquadratic term in the system's potential energy.

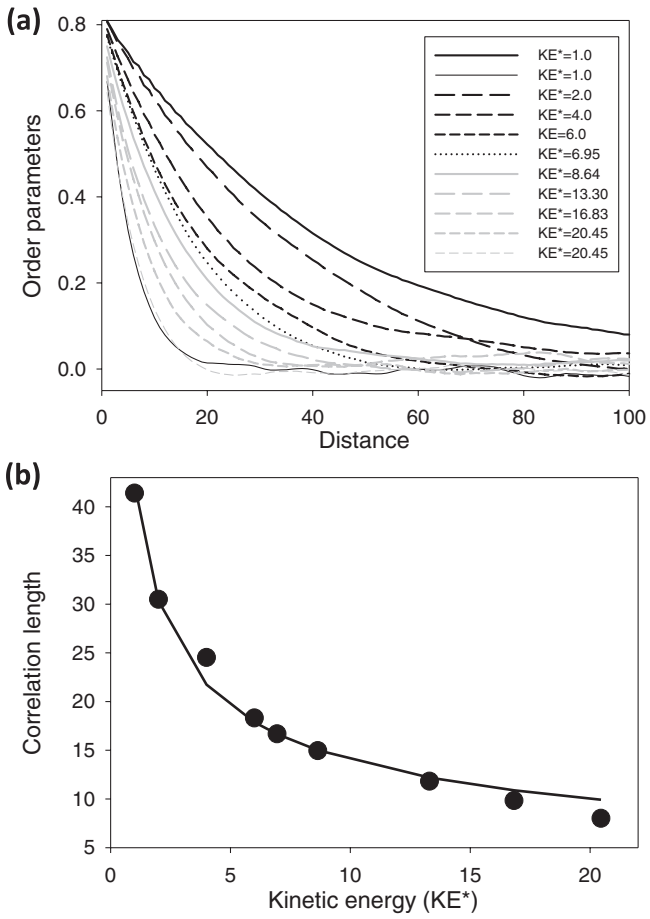

Figure 5. (a) String order parameter (thick lines) averaged over four annealed structures of the SO phase structures ($d = 0.005$) as a function of distance for various values of the kinetic energy KE^*. The range of string order correlation increases with decreasing temperature. The short range Néel order parameter (thin lines) at the two extreme values of kinetic energy show no significant temperature effect. (b) String order correlation length, ξ, as a function of kinetic energy. The uncertainty on the correlation length is estimated to be on the order of ± 2. The solid line is a best fit to the data in the form of a power law with critical exponent.

The Néel and string order parameters indicate the symmetries that are preserved or broken in the various identified phases. The example of the AF phase is a breaking of the translational symmetry of the system indicated by the non-zero value of the Néel order parameter. In the AF phase, if we know the sign of θ_i, then we also know the sign of θ_{i+1} and the signs of all angles in the system, hence the system is ordered and Z_2 symmetry is broken. Further, if we know the signs of θ_i and θ_j, then we know the signs of all angles in the system as evidenced by the non-zero value of the string order parameter and $Z_2 \times Z_2$ is also broken. As the b parameter is increased, the system enters the SL phase where the Néel and string order parameters go to zero with distance and the Z_2 and $Z_2 \times Z_2$ order is short range. In the SL phase, the two order parameters are practically equal so that the two types of order are of similar range. In the SO phase, the string order parameter exceeds the Néel order parameter for some distances, so that the $Z_2 \times Z_2$ order, while still local, is at larger distances than the Z_2 order itself. This disparity is what we refer to as the hidden order in our mechanical system. Finally, the D phase shows a rapid decrease of both the Néel and string order parameters to zero with distance showing that both the Z_2 and $Z_2 \times Z_2$ symmetries are not broken.

The effect of the magnitude of the kinetic energy of the system on the SO phase is illustrated in figure 5. The reduced kinetic energy is defined as $KE^* = \frac{KE}{I} = \frac{1}{2}\sum_{i=1}^{N}\left(\frac{\mathrm{d}\theta_i}{\mathrm{d}t}\right)^2$. The annealing protocol used to generate the SO phase given in figure 2(c) ($d = 0.005$) leads to $KE^* \sim 6.95\,\mathrm{s}^{-2}$ with small fluctuations resulting from conservation of the total energy. To achieve higher values of the kinetic energy, factors smaller than the factor of ten used previously are employed to decrease the angular velocities of the individual blocks at 2.95, and/or 2.975 million time steps. However, to achieve values of KE^* less than $6.95\,\mathrm{s}^{-2}$, we employed the standard angular momentum rescaling scheme which is imposed every time step after 3 million time steps. The total length of the simulation is therefore increased to 3.2 million steps to allow for additional relaxation time at low kinetic energy. In figure 5(a), we report the string order parameter ($d = 0.005$) as a function of distance averaged over four annealed structures for nine values of KE^*. In all cases, for all values of the kinetic energy, the number of sites supporting a zero remains reasonably consistent within $10\% \pm 1\%$ of the total number of sites. As the kinetic energy is lowered, disorder is lowered and the range of string order expands. We calculate a string order correlation length, ξ, by fitting O_{String} as a function of distance (l, in units of unit block or site spacing) to the exponentially decaying correlation function, $O_{\mathrm{String}}(d) = O_0 e^{-l/\xi}$. $\xi(KE^*)$ is reported in figure 5(b). We note that the prefactor O_0 depends only very weakly on the kinetic energy. The correlation length appears to diverge as KE^* decreases. We fit this data to a power law of the form $\xi(KE^*) = \xi_0 (KE^*)^{-\nu}$ and find $\xi_0 = 42.3$ and a critical exponent $\nu = 0.48$. This fit suggests that there is no critical kinetic energy and therefore no phase transition at finite kinetic energy. The critical exponent approaches the value of ½.

4. Conclusions

In summary, we have numerically studied a nonlinear dynamical mechanical system which exhibits four phases with respect to the Néel and string order parameters as a function of the strength of a biquadratic potential energy parameter, d. When this parameter is zero the signs of consecutive angles alternate, a phase similar to the antiferromagnetic order familiar in some magnetic materials. As d increases the perfect AF order is no longer evident at all distances but is only now a local order evidenced by the Néel and string order parameters which show agreement for this SL phase. As d again increases there is a range of parameters for which the Néel and string order parameters differ as a function of distance, the SO phase. Finally, at larger d, the system enters the D phase as both order parameters go to zero rapidly with distance.

The SO phase shows a type of hidden order as the string order parameters accounts for the correlation in the sign of two angles that are separated by a given distance. The range of correlation of the string order parameter increases with decreasing kinetic energy.

Examples of topological phases in classical systems have been known for some time. For instance, long-range order and topological order as well as their loss via Kosterlitz–Thouless transition have been discussed extensively in the context of melting in two-dimensions [19–23]. Similar behaviors have also been observed in a 2D photonic lattice using nonlinear optics [24]. However, the type of hidden order reported here has not previously been observed and quantified in a 1D dynamical mechanical system. The capacity to find classical behavior analogous to the hidden order that leads to quantum topological phases of matter opens new avenues to investigating these remarkable emergent phenomena. For instance, the extension to 2D frustrated mechanical systems is of prime interest. Our model marks a first step toward the theoretical and possible experimental study of emergent topological order in nonlinear mechanical systems defying characterization via local order parameters analogous to spin lattice systems.

Acknowledgments

We would like to thank Thomas Kennedy, Department of Mathematics at University of Arizona for reading the manuscript and providing useful comments.

ORCID iDs

P A Deymier https://orcid.org/0000-0002-1088-7958

References

[1] Deymier P A and Runge K 2017 *Sound Topology, Duality, Coherence and Wave-Mixing: An Introduction to the Emerging New Science of Sound* (*Springer Series in Solid State Sciences*) vol 188 (Berlin: Springer)
[2] Wang P, Lu L and Bertoldi K 2015 Topological phononic crystals with one-way elastic edge waves *Phys. Rev. Lett.* **115** 104302
[3] Rocklin D Z, Chen B G-g, Falk M, Vitelli V and Lubensky T C 2016 Mechanical Weyl modes in topological maxwell lattices *Phys. Rev. Lett.* **116** 135503
[4] Kumar Pal R and Ruzzene M 2017 Edge waves in plates with resonators: an elastic analogue of the quantum valley Hall effect *New J. Phys.* **19** 025001
[5] Chen X, Gu Z-C, Liu Z-X and Wen X-G 2013 Symmetry protected topological orders and the group cohomology of their symmetry group *Phys. Rev.* B **87** 155114
[6] Wen X-G 2017 Colloqium: zoo of quantum-topological phases of matter *Rev. Mod. Phys.* **89** 041004
[7] Haldane F D M 1983 Continuum dynamics of the 1-D Heisenberg antiferromagnet: identification with the O(3) nonlinear sigma model *Phys. Lett.* A **93** 464
[8] Haldane F D M 1983 Nonlinear field theory of large-spin heisenberg antiferromagnets: semiclassically quantized solitons of the one-dimensional easy-axis Néel state *Phys. Rev. Lett.* **50** 1153
[9] Wang P, Zheng Y, Fernandes M C, Sun Y, Xu K, Sun S, Kang S H, Tournat V and Bertoldi K 2017 Harnessing geometric frustration to form band gaps in acoustic channel lattices *Phys. Rev. Lett.* **118** 084302
[10] Kang S H, Shan S, Kosmtlj A, Noorduin W L, Shian S, Weaver J C, Clarke D R and Bertoldi K 2014 Complex ordered patterns in mechanical instability induced geometrically frustrated triangular cellular structures *Phys. Rev. Lett.* **112** 098701
[11] Hilker T A, Salomon G, Grusdt F, Omran A, Boll M, Demler E, Bloch I and Gross C 2017 Revealing hidden antiferromagnetic correlations in doped Hubbard chains via string correlators *Science* **357** 484
[12] Affleck I, Kennedy T, Lieb E H and Tasaki H 1987 Rigorous results on valence-bond ground states in antiferromagnets *Phys. Rev. Lett.* **59** 799
[13] Vasiliev A, Miroshnichenko A and Ruzzene M 2010 A discrete model and analysis of one-dimensional deformations in a structural interface with micro-rotations *Mech. Res. Commun.* **37** 225
[14] Vasiliev A, Miroshnichenko A and Ruzzene M 2008 Multifield model for Cosserat media *J. Mech. Mater. Struct.* **3** 1365
[15] Wang P, Casadei F, Shan S, Weaver J C and Bertoldi K 2014 Harnessing buckling to design tunable locally resonant acoustic metamaterials *Phys. Rev. Lett.* **113** 014301
[16] Schaeffer M and Ruzzene M 2015 Wave propagation in multistable magneto-elastic lattices *Int. J. Solids Struct.* **56–7** 78
[17] Gump J, Finkler I, Xia H, Sooryakumar R, Bresser W J and Boolchand P 2004 Light-induced giant softening of network glasses observed near the mean-field rigidity transition *Phys. Rev. Lett.* **92** 245501
[18] den Nijs M and Rommelse K 1989 Preroughening transitions in crystal surfaces and valence-bond phases in quantum spin chains *Phys. Rev.* B **40** 4709
[19] Halperin B I and Nelson D R 1978 Theory of two-dimensional melting *Phys. Rev. Lett.* **41** 121
[20] Nelson D R and Halperin B I 1979 Dislocation-mediated melting in two dimensions *Phys. Rev.* B **19** 2457
[21] Jaster A 2004 The hexatic phase of the two-dimensional hard disks system *Phys. Lett.* A **330** 120
[22] Kosterlitz J M and Thouless D J 1972 Long range order and metastability in two-dimensional solids and superfluids *J. Phys.* C **5** L124
[23] Kosterlitz J M and Thouless D J 1973 Ordering metastability, and phase transitions in two-dimensional systems *J. Phys.* C **6** 1181
[24] Small E, Pugatch R and Silberberg Y 2011 Berezinskii–Kosterlitz–Thouless crossover in a photonic lattice *Phys. Rev.* A **83** 013806